

# Group Re-identification via Transferred Single and Couple Representation Learning

Ziling Huang<sup>1</sup> Zheng Wang<sup>2,\*</sup> Shin'ichi Satoh<sup>2,3</sup> Chia-Wen Lin<sup>1</sup>

<sup>1</sup>National Tsinghua University <sup>2</sup>National Institute of Informatics <sup>3</sup>The University of Tokyo  
 huangziling@gapp.nthu.edu.tw; {wangz, satoh}@nii.ac.jp; cwlin@ee.nthu.edu.tw

**Abstract**—Group re-identification (G-ReID) is an important yet less-studied task. Its challenges not only lie in appearance changes of individuals which have been well-investigated in general person re-identification (ReID), but also derive from group layout and membership changes. So the key task of G-ReID is to learn representations robust to such changes. To address this issue, we propose a Transferred Single and Couple Representation Learning Network (TSCN). Its merits are two aspects: 1) Due to the lack of labelled training samples, existing G-ReID methods mainly rely on unsatisfactory hand-crafted features. To gain the superiority of deep learning models, we treat a group as multiple persons and transfer the domain of a labeled ReID dataset to a G-ReID target dataset style to learn single representations. 2) Taking into account the neighborhood relationship in a group, we further propose learning a novel couple representation between two group members, that achieves more discriminative power in G-ReID tasks. In addition, an unsupervised weight learning method is exploited to adaptively fuse the results of different views together according to result patterns. Extensive experimental results demonstrate the effectiveness of our approach that significantly outperforms state-of-the-art methods by 11.7% CMC-1 on the Road Group dataset and by 39.0% CMC-1 on the DukeMCMT dataset.

**Index Terms**—Group Re-identification, Unsupervised, Couple Representation

## I. INTRODUCTION

Due to the fast-growing applications in security and surveillance, person re-identification (ReID) has been drawing much attention [1], [2], [3], [4], [5]. While existing research works mainly focused on re-identifying individuals, searching out a group of multiple persons simultaneously was relatively rarely studied. In many practical applications identifying a group and then tracking and analyzing the group's behaviors and activities is of fundamental importance. Hence, re-identifying a group of persons (Group ReID or G-ReID) across cameras in different environments is getting more and more important. The G-ReID problem is different from the ReID problem from two perspectives. From the research perspective, G-ReID poses new challenging research problems (will be elaborated in the following) when the ReID target becomes a group of persons. These problems cannot be well addressed by existing individual ReID methods as reflected from the unsatisfactory performances of existing methods, and thus call for the development of novel group representations and solutions. From the application perspective, G-ReID is a powerful supplement

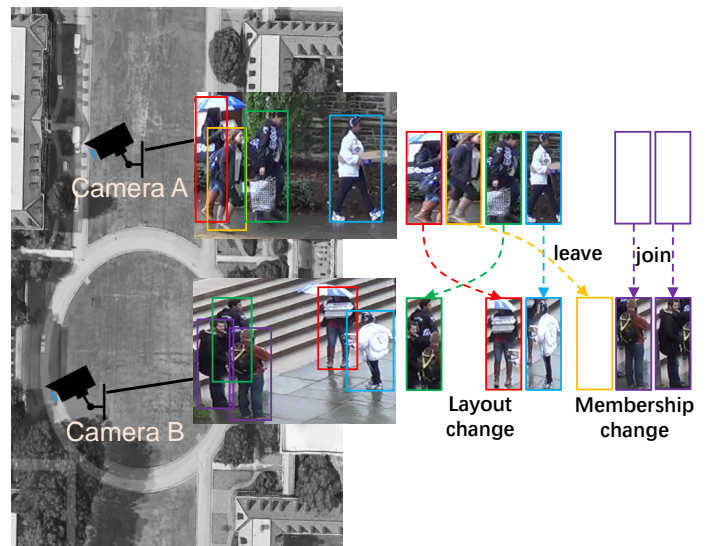


Fig. 1. Illustration of the challenges for G-ReID. Besides the challenge of the appearance change, G-ReID brings in the challenges of group layout and membership changes.

to individual ReID. For example, criminal cases are often conducted by a certain group of persons rather than an individual. Individual ReID techniques, however, often cannot identify a whole group of suspects in this application scenario. The technical challenges and practical values of G-ReID have attracted significant amounts of research efforts along this direction.

Different from ReID, G-ReID aims at associating a certain group across different cameras. Besides the challenge of appearance changes for individuals, such as low-resolution, pose variation, illumination variation, and blurred vision, G-ReID raises novel and unique challenges. 1) *Group layout change*. People in a group often change their locations under different camera views, as Figure 1 shows. 2) *Group membership change*. Also as illustrated in Figure 1, people will dynamically leave or join a group, thereby making the number of persons in the group change over time. To this end, it is usually not a good choice to treat the group as a whole to extract its global/semi-global features as [6] did, because the temporal dynamics in a group's group layout and membership will alter the visual content of the group. 3) *Lack of labelled training data*. In addition, G-ReID is a new task and lacks

\* Corresponding Author

annotated image samples with group IDs, *i.e.*, the number of group images is too few to learn robust group representations. We list a comparison of ReID and G-ReID as shown in Table I.

TABLE I  
COMPARISON OF THE CHALLENGES IN REID AND G-REID

Challenge	ReID	G-ReID
Appearance Change	✓	✓
Layout Change	×	✓
Membership Change	×	✓
Training Set	Abundant	No

Based on the considerations above, We focus on the two most challenging problems in G-ReID: 1) the problem of scarce training data, and 2) the problem of layout and membership changes and propose the following new representation learning schemes:

**Transferred Single Representations:** Since global features cannot well represent dynamically varying contents in a group, we consider to use single person features to perform group matching as a group image can be treated as a collection of multiple subimages of individual group members. The reason behind is that if we find corresponding persons in a target group, we will search out the target group as well. Considering that training data is difficult to acquire, [7] exploited hand-crafted features to represent individuals in a group. Nevertheless, hand-crafted representations usually cannot effectively address the appearance change problem in G-ReID due to changes in environments and video capturing conditions. As we know, there exist rich amounts of training datasets suitable for general ReID, which motivates us to make use of existing labeled ReID samples to learn single-person representations. However, the domain gap between the ReID training datasets and target G-ReID images often cause severe performance drop. Therefore, to compensate for the domain shift, we need to find a way to transfer the model learned from existing ReID datasets to better represent new individuals in target G-ReID images. Inspired by [8], [9], we propose to transfer the image style of a ReID dataset to that of target G-ReID dataset while preserving individuals’ identities. In this way, representative features of individuals in a group can be properly extracted by our transferred representation model.

**Transferred Couple Representations:** In G-ReID, we can obtain additional useful information from neighboring group members. Because of group membership changes, it is difficult to exactly determine how many persons are in a group. Regardless of the number of persons in a group, the group can be represented as multiple couple relations. For example, if a group contains three persons  $A$ ,  $B$  and  $C$ , their couple relations expressed as  $A - B$ ,  $A - C$  and  $B - C$  can be used as effective features for identifying a target group. As a result, we can search out a target group by finding a best-match with the group’s corresponding couple relations. Based on this consideration, we propose a couple representation learning network to leverage the information of neighboring individuals. The couple representation learning can also benefit from the proposed domain-transfer technique mentioned

above. Note that, in a group, all members can be represented as multiple one-to-one relations (couple representations). Triplet or batch relations can be also represented by multiple one-to-one relations. That is why we choose the couple representation, which is the simplest unit for social relationship.

Based on the above discussions, we propose a Transferred Single and Couple Representation Learning Network (TSCN), that can offline learn effective features for representing single members and couple relations in a group. We also propose an online feature fusion method to adaptively combine the two kinds of features together to obtain better group representations. Inspired by [10], our method learns the weights for fusing the single representations and couple representations without supervision. As will be shown below, our method is easy to implement, yet effective. Furthermore, the simplicity of our method makes it easy to be applied to different target domains, which is usually not the case for sophisticated methods.

Our contributions lie in the following three aspects:

- To tackle the scarce training data problem, we are among the first to propose style-transferring rich collections of individual ReID samples to the target domain of group ReID to enrich the training samples.
- We further propose a novel couple representation to capture the social relationship in a group to well address the problem of layout and membership changes for the first time.
- We propose an online fusion method to adaptively combine the learned single and couple representation results together for better group re-identification. Extensive experimental results confirm a performance leap from the relevant state-of-the-art techniques in the area.

The rest of this paper is organized as follows. Some most relevant works are surveyed in Sec. II. Sec. III presents the proposed schemes for transferred representation learning, couple representation learning, and feature fusion. In Sec. IV, experimental results are demonstrated. Finally, conclusions are drawn in Sec. V.

## II. RELATED WORKS

**Deep learning based ReID.** Deep learning-based approaches have been extensively studied in general ReID field. For example, Li *et al.* [11] proposed a filter pairing neural network to jointly handle misalignment and geometric transforms. In order to learn features from multiple domains, Xiao *et al.* [12] utilized a domain-guided dropout algorithm to improve the feature learning procedure. Moreover, the method proposed in [13] makes full use of human part cues to alleviate pose variations and learn robust representations from both a whole image and its different local parts. Chen *et al.* [14] formulated a unified deep ranking framework that jointly maximizes the strengths of features and metrics. Zhu *et al.* [15] integrated spatial information for discriminative visual representations by partitioning a pedestrian image into horizontal parts, and proposed a part-based deep hashing network. Yao *et al.* [16] proposed a part loss network, to minimize both the empirical classification risk on training

person images and the representation learning risk on unseen person images. Zheng *et al.* [17] introduced pose-invariant embedding as a pedestrian descriptor and designed a PoseBox fusion CNN architecture. The descriptor is thus defined as a fully connected layer of the network for the retrieval task. However, these supervised learning-based works all require abundant labeled training data. Moreover, all of these works mainly focused on individual person re-identification. None of them paid attention to G-ReID with very limited training data.

**G-ReID.** Recently, relatively fewer works have focused on G-ReID tasks [18], [6], [19], [20], [7], compared to general ReID tasks. Some of them mainly attempted to extract global or semi-global features. For example, Cai *et al.* [18] proposed a discriminative covariance descriptor to obtain both global and statistical features. Zheng *et al.* [19] proposed semi-global features by segmenting a group image into several ring regions. Since persons in a group often change their locations under different views (*i.e.*, layout-change), global and semi-global features are usually sensitive to such changes. In order to make use of individuals' features in the groups, Zhu *et al.* [20] introduced patch matching between two group photos. However, it requires prior restrictions on vertical misalignments, making it unworkable under certain circumstances. Xiao *et al.* [7] leveraged multi-grain information and attempted to fully capture the characteristics of a group. This approach, however, involves too much redundant information and employs common hand-crafted features, thereby making its accuracy not satisfactory enough.

**Domain transfer.** Recently, Generative Adversarial Networks (GANs) have been applied to transfer image styles from a source domain to a target domain [21], [22], [23], [24], [25]. Gatys *et al.* [21] separated the image content and image style apart and recombined them afterwards, so that the style of one image can be transferred into another. Taigman *et al.* [24] proposed a domain transfer network to translate images to another domain while preserving original identities. By making use of the existing domain-transfer techniques, we are able to take advantage of the abundant ReID datasets to improve the performance of our method.

### III. TRANSFERRED SINGLE AND COUPLE REPRESENTATION LEARNING

In a G-ReID task, we have a probe image  $p$  containing a group of  $N$  persons, in which the  $i$ -th person in the group is denoted  $p^i$ . We aim at finding the corresponding group of probe image  $p$  in gallery images  $\mathcal{G} = \{g_t\}$ , where  $g_t$  represents the  $t$ -th group image in gallery  $\mathcal{G}$ . Let  $g_t^j$  denote the  $j$ -th person in group image  $g_t$ . As depicted in Figure 2, the proposed framework consists of three major parts. First, a domain transfer method is used to transfer the styles of the training ReID dataset into that of the target G-ReID images. In the offline Representation Learning step, we train the Transferred Single and Couple Network (TSCN) on the domain-transferred dataset. In the Online fusion step, the features extracted by the Single Representation Learning Network and the Couple Representation Learning Network are adaptively fused so that one group can be more accurately identified by using the fused single and couple representations.

#### A. Domain Transfer

Because the total number of people in a collection of G-ReID images is usually rather limited, it is difficult to train a useful network directly based on those data themselves. To learn better representations, we should make use of external information. There exists a rich collection of ReID datasets which can be used to train good feature representations. Nevertheless, the domain gap between the existing ReID datasets and the target G-ReID images, that is caused by their different capturing conditions, can significantly degrade the effectiveness of representation learning. To address this problem, given a training ReID dataset  $\mathcal{S} = \{s_i\}_{i=1}^{N_s}$ , we propose utilizing domain transfer to learn a mapping function  $G : \mathcal{S} \rightarrow \mathcal{G}$  from the style of ReID dataset  $\mathcal{S}$  to that of G-ReID dataset  $\mathcal{G}$  so that the distribution of  $G(\mathcal{S})$  can be indistinguishable from that of dataset  $\mathcal{G}$ . In our work, we exploit the CamStyle<sup>1</sup> method [9], to generate the dataset  $G(\mathcal{S})$  from the dataset  $\mathcal{S}$ .

In this way, the dataset  $G(\mathcal{S})$ , where  $y_k^s \in G(\mathcal{S})$  denotes the  $k$ -th image of the  $s$ -th person in the dataset, can be used to train the Single Representation Learning Network (SRLN)  $\mathcal{F}_{sin}$ . In addition, we construct co-occurrence relations  $r^{s_1 s_2} = \{(y_{k_1}^{s_1}, y_{k_2}^{s_2}) | s_1, s_2 = 1, \dots, N_s, k_1 = 1, \dots, N_{s_1}, k_2 = 1, \dots, N_{s_2}, s_1 \neq s_2\}$  between pairs of persons. These co-occurrence relations are used to train the Couple Representation Learning Network (CRLN)  $\mathcal{F}_{cou}$ .

The two networks are then respectively used to extract the single and couple features of gallery images  $g_t$  and probe image  $p$ . For probe image  $p$ , let  $\mathcal{F}_{sin}(p^i)$  and  $\mathcal{F}_{cou}(p^{i_1 i_2})$  respectively represent its single and couple features, where  $p^{i_1 i_2} = \{(p^{i_1}, p^{i_2}) | i_1, i_2 = 1, \dots, N, i_1 \neq i_2\}$  denote the relations of the probe. For gallery image  $g_t$ , its single and couple features are respectively represented as  $\mathcal{F}_{sin}(g_t^j)$  and  $\mathcal{F}_{cou}(g_t^{j_1 j_2})$ , where  $g_t^{j_1 j_2} = \{(g_t^{j_1}, g_t^{j_2}) | j_1, j_2 = 1, \dots, N_t, j_1 \neq j_2\}$  denote the relations of the gallery.

#### B. Offline Representation Learning Framework

The offline Representation Learning Framework is divided into two parts: SRLN for extracting single-person features, and CRLN for extracting joint features between two members in a group. We select ResNet-50 as the backbone CNN structure, since it is the most popular CNN network used in general ReID. Detailed settings about training the network are presented in the experiment section.

In order to match a group in a collection of group images, the most straightforward method is to find every corresponding people between two groups. We take advantage of an abundance of existing ReID datasets  $G(\mathcal{S}) = \{y_k^s\}$  to train the SRLN  $\mathcal{F}_{sin}$ , for which two loss terms are used in the loss function: a cross-entropy loss for classification and a triplet loss for similarity learning.

For G-ReID, besides personal features of individual group members, the joint features between two co-appearing members are also useful as the co-occurrences of group members has proven to be an effective feature for characterizing the

<sup>1</sup>We refer to the code <https://github.com/zhunzhong07/CamStyle>.

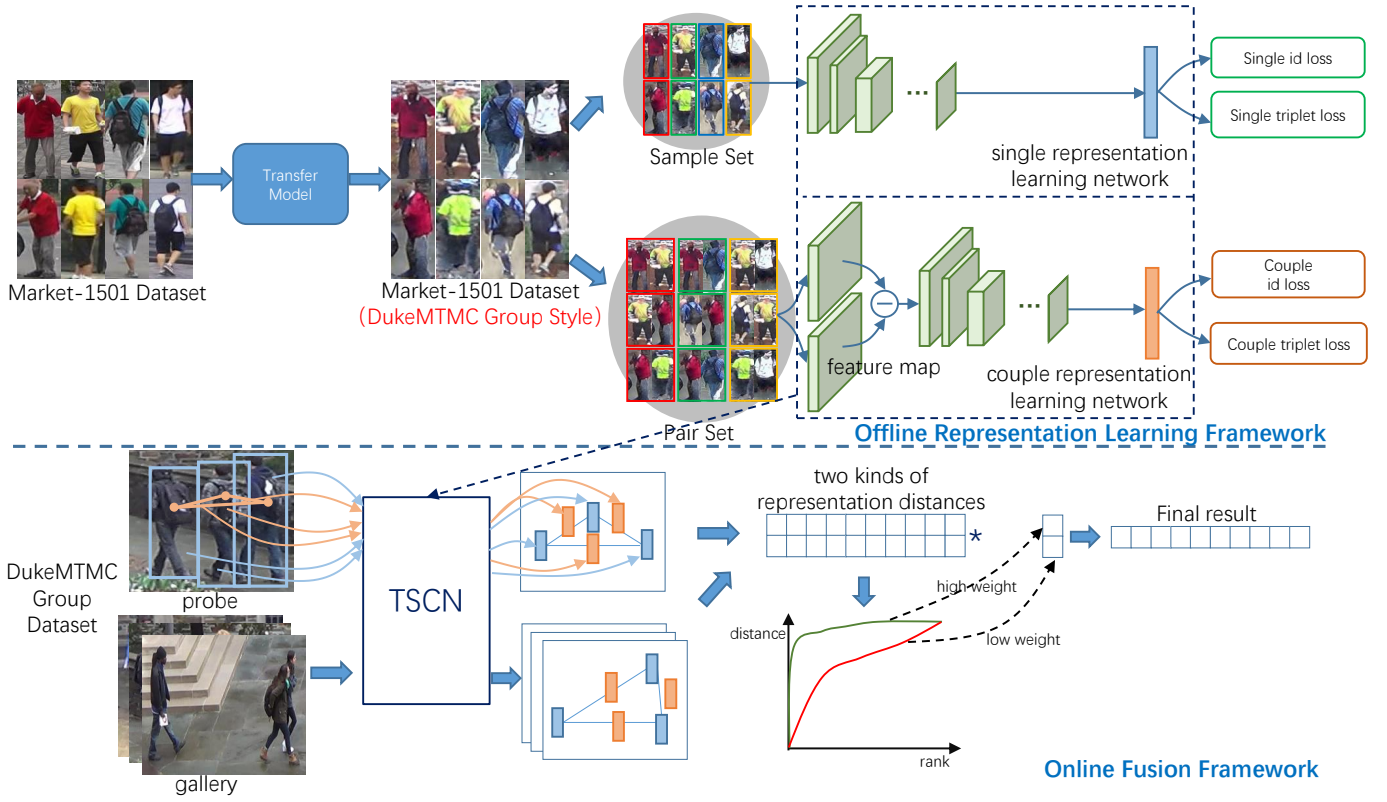


Fig. 2. **Proposed architecture.** The proposed architecture consists of two parts: the offline representation learning framework and the online fusion framework. Here, we take DukeMTMC group dataset as the example target-domain dataset. In offline representation learning, we first transfer the style of source-domain dataset (e.g., Market-1501) to that of the target one (e.g., DukeMTMC). We then train the Transferred Single and Couple Network (TSCN) on the transferred labeled dataset. During online fusion, TSCN extracts multiple single and couple features from each group image, and then measure the single and couple representation distance compared to the representations of gallery groups. Through evaluating the “L” shape fitness of the curves, we learn the weights for combination. Finally, the fusion results are obtained according to the weights.

social relationship in a group [26], [27]. As we know, no matter how many people in an group, they can always be represented as relations between every two group members. In our work, we focus on the relations between two members co-occurring in a group regardless of their spatial distance in the group image as they often change their locations in a group dynamically under different camera views. Based on the above discussion, we propose to represent the couple relations between every two group members by the difference of their personal features to compactly signify the co-occurrence of the two members with only their discrepancy, since the subtraction operation removes their common features. By contrast, the co-occurrence of group members can also be represented by other operations like addition and concatenation. However, adding two person’s features magnifies their common features so as to make the representations less discriminative, whereas concatenation doubles the number of parameters, thereby significantly increasing the complexity of network training.

Based on the above considerations, the goal of the CRLN  $\mathcal{F}_{cou}$  is to learn effective occurrence representations of couple pairs of members in a group. To this end, after extracting the features of individual members by the SRLN, the CRLN then pairs all two-member couples in the  $G(S)$ , and for each couple of two members, subtracts one member’s features from the other’s to represent their co-occurrence features  $r^{s_1s_2}$ . Similar

to SRLN, a loss function involving a cross-entropy loss term for classification and a triplet loss term for similarity learning is used to train the CRLN.

Rather than using the original group member labels, we assign new labels for our relationship dataset based on Equation (1):

$$\ell(i, j) = -(c - j) + \sum_{t=1}^i (c - t) \quad (1)$$

where  $i$  and  $j$  denote the original labels in  $G(S)$ , and  $c$  denotes the total number of persons in  $G(S)$ . The couple features  $r^{s_1s_2}$  along with their associated labels are used to train  $\mathcal{F}_{cou}$  to learn the relation representations between every two co-occurring persons. For example, suppose we have three identities 1, 2, 3 in the ReID dataset. The relation ID between samples from person 1 and from person 2 is obtained as  $\ell(1, 2) = -(3 - 2) + 3 - 1 = 1$ , the relation ID between the samples from person 1 and from person 3 is obtained as  $\ell(1, 3) = -(3 - 3) + 3 - 1 = 2$ , and the relation ID between the samples from person 2 and from person 3 are obtained as  $\ell(2, 3) = -(3 - 3) + 3 - 2 + 3 - 1 = 3$ .

### C. Online Fusion Framework

Since the proposed TSCN extracts both individuals’ features and pairs’ features, the two kinds of features need to be

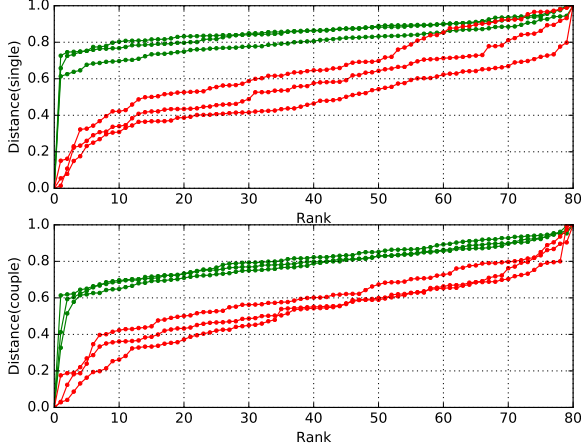


Fig. 3. **Logarithmic rank-distance curves for different probes.** Each curve indicates all the distances (sorted in the ascending order) of the corresponding probe and all the gallery groups. The top figure shows the results with single features, while the bottom one is generated using couple features. Note that the green lines indicate the representations achieving a good retrieval accuracy, whereas the red lines indicate low-accuracy ones. All the high-accuracy curves (*i.e.*, the features are discriminative) are L-shaped, but the property does not hold for the low-accuracy curves.

adequately fused to obtain better representations for G-ReID. Inspired by [10] that demonstrated that for traditional ReID the rank-distance curve between a probe image and all gallery images sorted in the ascending order exhibits an “L” shape provided that the learned representations are discriminative; otherwise, the L-shape property does not hold with non-discriminative representations. The L-shape property means that there exists a turning point at which the rank-distance curve is significantly flattened out. This property gives a clue for finding a way of fusing the two kinds of features in TSCN. However, since our work focuses on G-ReID rather than individual ReID, we need make sure if the L-shape property still holds in G-ReID tasks.

Let  $\{\mathcal{F}_{sin}(p^i)\}_{i=1}^N$  denote the single features of all individuals in a probe image and  $\{\mathcal{F}_{sin}(g_t^j)\}_{j=1}^{N_t}$  the features of all individuals in the  $t$ -th gallery image  $g_t$ . The distance between probe image  $p$  and gallery image  $g_t$  is defined as

$$d_t^{sin} = \frac{1}{N} \sum_{i=1}^N \min \{D(\mathcal{F}_{sin}(p^i), \mathcal{F}_{sin}(g_t^j)) | j = 1, 2, \dots, N_t\} \quad (2)$$

where  $D(\cdot)$  denotes the distance metric (say, Euclidean distance in this work). Similarly, we also calculate the couple distance  $d_t^{cou}$  between probe image  $p$  and gallery image  $g_t$  by replacing the single features with the couple features in Equation (2).

The logarithmic rank-distance curves are shown in Figure 3. The green curves indicate the matching distances with discriminative features, whereas the red ones indicate the matching distances with poor features. Obviously, the green curves are L-shaped, while the red ones are not. Besides, the green curves enclose relatively large areas compared with the red ones.

Based on these observations, we propose to fuse the single and couple features to obtain the final distance by using the following weighted sum:

$$d_t^{total} = w^{sin} \times d_t^{sin} + w^{cou} \times d_t^{cou} \quad (3)$$

where the weights are determined by the enclosed areas of the distance curves with the single and couple features, respectively:

$$w = e^{\sum_r d_t} \quad (4)$$

where  $r$  denotes the rank (*i.e.*, the x-axis of the the curves in Figure 3). The higher the enclosed area, the more discriminative the features, and the larger the weight.

Based on Equation (2), the best-match group image in the gallery will lead to the smallest feature distance and the remaining will lead to larger distances. Therefore, the best-match gallery image can be identified by searching for that with the lowest matching distance  $d_p$ :

$$d_p = \min\{d_t^{total} | t = 1, 2, \dots, N_t\} \quad (5)$$

## IV. EXPERIMENTAL RESULTS

### A. Datasets and Experiment Setting

**Datasets.** Our method is evaluated on two public G-ReID datasets available in [7]. Some examples are shown in Figure 4. The **DukeMTMC Group** dataset contains 177 group image pairs selected from a 8-camera-view DukeMTMC dataset [28]. The **Road Group** dataset contains 162 group pairs taken from a two-camera crowd road scene. These two datasets both include severe object occlusions and large layout & group membership changes. Following [7], half of each dataset is evaluated under the protocol in [20], and the Cumulative Matching Characteristic (CMC) metrics [7] are used for performance evaluation. Moreover, we define two cross-view groups as the same one when they have more than 60% members in common.

We also use the Market-1501 dataset [29] as the source-domain ReID dataset due to its large amount of training instances: 15,936 images for 751 individuals. In our work, we transfer the Market-1501 dataset to the styles of **DukeMTMC Group** and **Road Group**, respectively, as illustrated in Figure 4.

**Setting for Style Transfer.** In our work, we transfer the style of existing ReID datasets to the target G-ReID datasets (*e.g.*, **DukeMTMC Group** and **Road Group**), prior to training the representations. We use the CycleGAN [30] to transfer the style for each target G-ReID dataset. As a result, we obtain the DukeMTMC-style Market-1501 dataset and the Road-style Market-1501 dataset. In the training stage, we resize all input images to  $256 \times 256$  and use the Adam optimizer. The batch size is 10, and the learning rates are 0.0002 and 0.0001, respectively, for the Generator and the Discriminator.

**Setting for CNN Models.** In both SRLN and CRLN, the ResNet-50 with two additional fully connected layers is used as the backbone. The learning rate is set to 0.01, and the dropout probability is set to 0.5. The input images are resized to  $256 \times 128$ . We use the SGD solver to train the CNN model

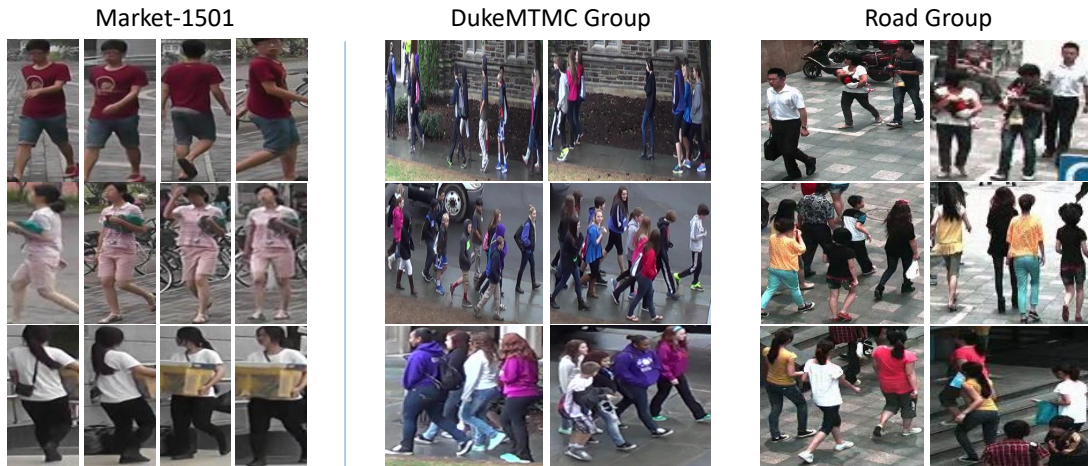


Fig. 4. Snapshots of the utilized datasets. From left to right, the datasets are respectively **Market-1501** (ReID), **DukeMTMC Group** and **Road Group** (G-ReID). Each row of each dataset shows a few snapshots with the same person/group ID.

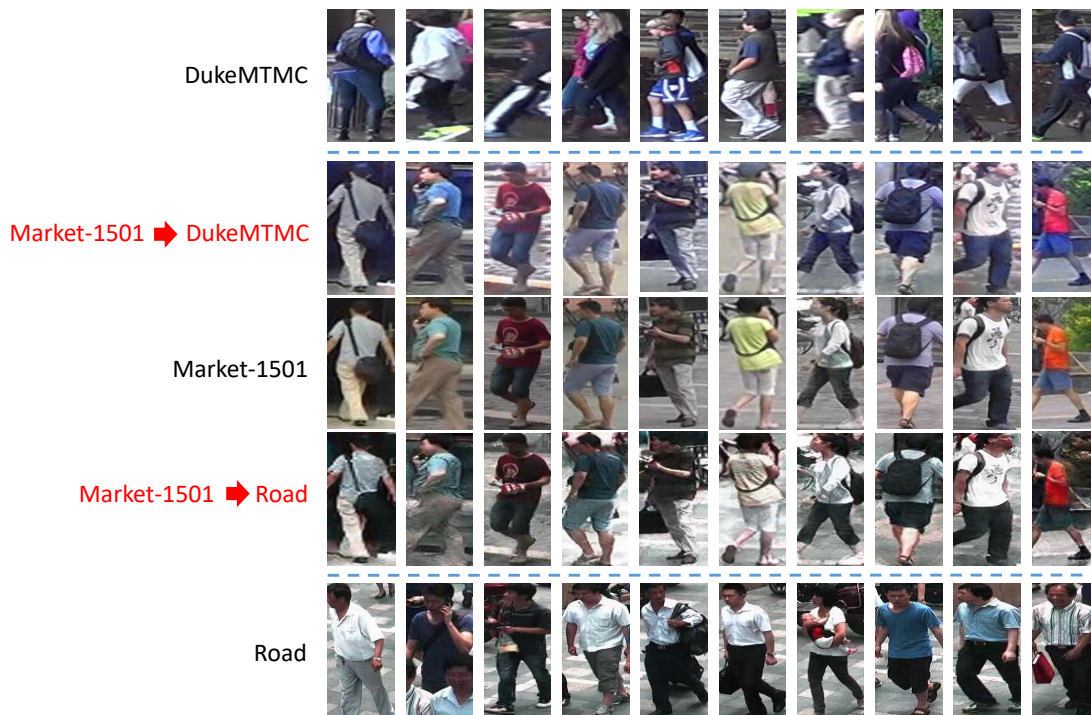


Fig. 5. Snapshots of style-transferred samples. The images in the third row are from the source domain **Market-1501**. The images in the first and fifth rows are cropped respectively from the target domain **DukeMTMC Group** and **Road Group**. The second row shows the generated images with **DukeMTMC** style, and the fourth row shows the generated images with **Road** style.

TABLE II

EVALUATION OF THE TRANSFERRED REPRESENTATION LEARNING ON THE DUKEMTMC AND ROAD GROUP DATASETS. THE SUFFIX ‘S’ INDICATES THE SINGLE REPRESENTATION, AND THE SUFFIX ‘C’ INDICATES THE COUPLE REPRESENTATION. THE ABBREVIATION ‘TR.’ DENOTES TRANSFER LEARNING. MGR IS THE STATE-OF-THE-ART METHOD COMPARED

Method	DukeMTMC Group				Road Group			
	CMC-1	CMC-5	CMC-10	CMC-20	CMC-1	CMC-5	CMC-10	CMC-20
MGR	47.4	68.1	77.3	87.4	72.3	90.6	94.1	97.5
TSCN(s) w/o TR.	75.0	83.0	89.8	94.3	80.2	90.1	92.6	<b>98.8</b>
TSCN(s) w/ TR.	<b>80.7</b>	<b>89.8</b>	<b>94.3</b>	<b>96.6</b>	<b>82.7</b>	<b>93.8</b>	<b>96.3</b>	<b>98.8</b>
TSCN(c) w/o TR.	50.0	80.7	85.2	95.5	50.6	74.1	80.2	87.7
TSCN(c) w/ TR.	<b>62.5</b>	<b>83.0</b>	<b>89.8</b>	<b>95.5</b>	<b>70.4</b>	<b>79.0</b>	<b>84.0</b>	<b>90.1</b>

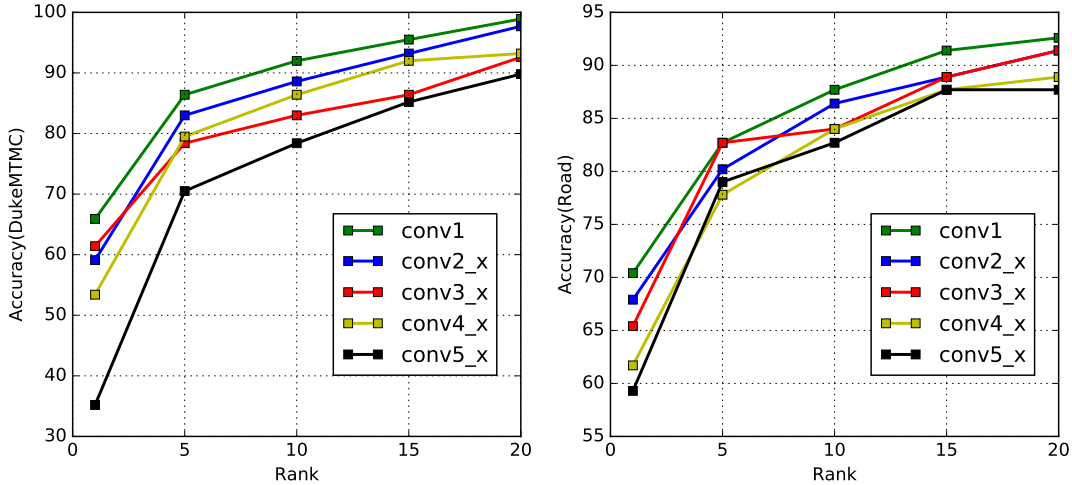


Fig. 6. **Effect of the selection of the subtraction layer for couple representation learning.** The curves show the re-identification accuracy results of different designs of subtraction layers. The two figures respectively show the results (CMC-1) on DukeMTMC and Road Group on **DukeMTMC Group** and **Road Group**, respectively.

and set the batch-size to 24. To avoid data unbalanced, we choose 100 identities from the transferred dataset, where each identity contains 14 – 16 samples. If we use identity 1 and identity 2 to form paired samples for a couple class, which contain  $C1$  and  $C2$  samples respectively, we can generate  $C1 \times C2$  paired samples for training.

### B. Performance of Transferred Representation Learning

In this subsection, we conducted experiments to show the effectiveness of transferred representation learning, respectively exploiting the single representations and couple representations. To show the effectiveness of transfer training, we conducted the representation learning by **Market-1501** with/without a transferred style, respectively. For the testing G-ReID datasets, we exploited DukeMTMC/Road samples as the transfer target domain samples. Some examples of style-transferred samples are shown in Figure 5.

Table II shows the CMC results of the single and couple representations with/without transferred sample learning. From the table, we find that the non-transferred results, *i.e.*, ‘TSCN(s) w/o TR.’ and ‘TSCN(c) w/o TR.’ beat all the state-of-the-art results, as the features learned by the CNN are significantly better than the hand-crafted features in representing a group. We can also observe that the transferred representation learning (*i.e.*, ‘TSCN(s) w/ TR.’ and ‘TSCN(c) w/ TR.’) outperforms the non-transferred learning ones. The single representation learning achieves 5.7% and 2.5% CMC-1 accuracy improvements on **DukeMTMC Group** and **Road Group**, respectively. The couple representation learning achieves 12.5% and 19.8% CMC-1 accuracy improvements on **DukeMTMC Group** and **Road Group**, respectively.

### C. Performance of Couple Representation Learning

The CRLN is constructed by the Resnet-50 network pre-trained on the transferred data. We divided Resnet-50 into six parts based on [31]. The difference of the feature maps

of different parts can be obtained by subtraction, and is then sent to the rest of the network. The output of the full-connected layer is taken as the couple representations. The results on the dataset are shown in Figure 6. From Figure 6, we can make a conclusion that if the feature map subtraction is placed closer to the front (conv1), we can obtain better results. That is, the CRLN performs better in representing the relations of low-level feature maps, rather than in the high-level individual features. Figure 7 shows some examples in which couple representations are more discriminative than single representations.

Here we also compare the couple representations formed by (1) subtraction operation ‘TSCN(c) SUB.’ and (2) addition operation ‘TSCN(c) ADD.’. Table III shows that the proposed couple representations ‘TSCN(c) SUB.’ outperform the couple representations obtained by addition operation ‘TSCN(c) ADD.’. The results demonstrate the effectiveness of the proposed couple representations by the difference of feature maps.

### D. Performance of Fusion

Here we compare the proposed adaptive feature fusion ‘TSCN AD.’ of single and couple representations with (1) equal-weight feature fusion ‘TSCN EQ.’, (2) transferred single representations only ‘TSCN(s) w/ TR.’, and (3) transferred couple representations only ‘TSCN(c) w/ TR.’. Table IV shows that the adaptive fusion scheme presented in Section III-C outperforms the other compared methods in all CMC metrics. In contrast, the equal-weight fusion performs the same with transferred single representations on **DukeMTMC Group**, but slightly worse on **Road Group**. The results demonstrate the effectiveness of the adaptive weighting scheme guided by the enclosed areas of the rank-distance curves associated with the single and couple features.

TABLE III

PERFORMANCE EVALUATION OF DIFFERENT COUPLE REPRESENTATIONS RESPECTIVELY CONSTRUCTED BY SUBTRACTION AND ADDITION ON THE DUKEMTMC AND ROAD GROUP DATASETS. THE ABBREVIATION ‘ADD.’ MEANS THE COUPLE REPRESENTATIONS CONSTRUCTED BY PERFORMING ADDITION ON FEATURE MAPS, AND ‘SUB.’ MEANS THE COUPLE REPRESENTATIONS CONSTRUCTED BY PERFORMING SUBTRACTION ON FEATURE MAPS

Method	DukeMTMC Group				Road Group			
	CMC-1	CMC-5	CMC-10	CMC-20	CMC-1	CMC-5	CMC-10	CMC-20
TSCN(c) ADD.	44.3	56.8	80.7	86.4	48.1	70.4	79.0	88.9
TSCN(c) SUB.	<b>62.5</b>	<b>83.0</b>	<b>89.8</b>	<b>95.5</b>	<b>70.4</b>	<b>79.0</b>	<b>84.0</b>	<b>90.1</b>

TABLE IV

PERFORMANCE EVALUATION ON DIFFERENT FUSION METHODS ON THE DUKEMTMC AND ROAD GROUP DATASETS. THE SUFFIX ‘S’ REPRESENTS THE SINGLE REPRESENTATIONS, AND THE SUFFIX ‘C’ REPRESENTS THE COUPLE REPRESENTATIONS. THE ABBREVIATION ‘TR.’ DENOTES TRANSFER LEARNING, ‘EQ.’ DENOTES THE FUSION RESULTS OBTAINED WITH EQUAL WEIGHTS, AND ‘AD.’ DENOTES THE FUSION RESULTS OBTAINED WITH ADAPTIVE WEIGHTS BY EQUATION (3)

Method	DukeMTMC Group				Road Group			
	CMC-1	CMC-5	CMC-10	CMC-20	CMC-1	CMC-5	CMC-10	CMC-20
TSCN(s) w/ TR.	80.7	89.8	94.3	96.6	82.7	93.8	<b>96.3</b>	<b>98.8</b>
TSCN(c) w/ TR.	62.5	83.0	89.8	95.5	70.4	79.0	84.0	90.1
TSCN EQ.	80.7	89.8	94.3	96.6	82.7	90.1	92.6	95.1
TSCN AD.	<b>86.4</b>	<b>98.8</b>	<b>98.8</b>	<b>98.8</b>	<b>84.0</b>	<b>95.1</b>	<b>96.3</b>	<b>98.8</b>

TABLE V

COMPARISON WITH THE STATE-OF-THE-ART G-REID METHODS ON THE DUKEMTMC AND ROAD GROUP DATASETS

Method	DukeMTMC Group				Road Group			
	CMC-1	CMC-5	CMC-10	CMC-20	CMC-1	CMC-5	CMC-10	CMC-20
CRRRO-BRO	9.9	26.1	40.2	64.9	17.8	34.6	48.1	62.2
Covariance	21.3	43.6	60.4	78.2	38.0	61.0	73.1	82.5
PREF	22.3	44.3	58.5	74.4	43.0	68.7	77.9	85.2
BSC+CM	23.1	44.3	56.4	70.4	58.6	80.6	87.4	92.1
MGR	47.4	68.1	77.3	87.4	72.3	90.6	94.1	97.5
TSCN (Ours)	<b>86.4</b>	<b>98.8</b>	<b>98.8</b>	<b>98.8</b>	<b>84.0</b>	<b>95.1</b>	<b>96.3</b>	<b>98.8</b>



Fig. 7. Examples showing the effectiveness of couple representations. The first column shows the probe image. The following columns show the top three matches. ‘Single’ and ‘Couple’ indicate that the results are obtained respectively by the single or couple representation learning.

### E. Comparison with State-of-the-art Methods

Table V shows the results of a few state-of-the-art methods on **DukeMTMC Group** and **Road Group**. The compared methods include CRRO-BRO [19], Covariance [18], PREF [6], BSC+CM [20] and MGR [7]. The results show that our method outperforms all existing G-ReID methods and achieves significant improvements, thanks to the proposed transferred representation learning and adaptive feature fusion. In particular, compared with the best state-of-the-art method, our method achieves improvements by 11.7% CMC-1 on **Road Group** and 39.0% CMC-1 on **DukeMTMC Group**.

## V. CONCLUSION

In this paper, we addressed an important but rarely studied problem: group re-identification. We have proposed a transferred representation learning and a couple representation learning scheme to respectively overcome the two major challenges with group re-identification: the limited training data challenge and the membership and layout change challenge. We have also propose an adaptive fusion method to fuse the single and couple representation results for better group re-identification. The experimental results have confirmed a

performance leap from the relevant state-of-the-art techniques in the area.

## REFERENCES

- [1] Y.-C. Chen, W.-S. Zheng, and J. Lai, "Mirror representation for modeling view-specific transform in person re-identification," in *Inte. Joint Conf. Artificial Intell.*, 2015, pp. 3402–3408.
- [2] S. Li, M. Shao, and Y. Fu, "Cross-view projective dictionary learning for person re-identification," in *Int. Joint Conf. Artificial Intell.*, 2015, pp. 2155–2161.
- [3] Z. Wang, R. Hu, C. Liang, Y. Yu, J. Jiang, M. Ye, J. Chen, and Q. Leng, "Zero-shot person re-identification via cross-view consistency," *IEEE Trans. Multimedia*, vol. 18, no. 2, pp. 260–272, 2016.
- [4] Z. Wang, R. Hu, Y. Yu, J. Jiang, C. Liang, and J. Wang, "Scale-adaptive low-resolution person re-identification via learning a discriminating surface," in *Int. Joint Conf. Artificial Intell.*, 2016, pp. 2669–2675.
- [5] W. Li, X. Zhu, and S. Gong, "Person re-identification by deep joint learning of multi-loss classification," in *Int. Joint Conf. Artificial Intell.*, 2017, pp. 2194–2200.
- [6] G. Lisanti, N. Martinel, A. Del Bimbo, and G. Luca Foresti, "Group re-identification via unsupervised transfer of sparse features encoding," in *Int. Conf. Comput. Vis.*, 2017, pp. 2449–2458.
- [7] H. Xiao, W. Lin, B. Sheng, K. Lu, J. Yan, J. Wang, E. Ding, Y. Zhang, and H. Xiong, "Group re-identification: Leveraging and integrating multi-grain information," in *ACM Conf. Multimedia*, 2018, pp. 192–200.
- [8] Z. Zhong, L. Zheng, S. Li, and Y. Yang, "Generalizing a person retrieval model hetero-and homogeneously," in *European Conf. Comput. Vis.*, 2018, pp. 172–188.
- [9] Z. Zhong, L. Zheng, Z. Zhong, S. Li, and Y. Yang, "Camera style adaptation for person re-identification," in *IEEE Conf. Comput. Vis. Pattern Recognit.*, 2018, pp. 5157–5166.
- [10] L. Zheng, S. Wang, L. Tian, F. He, Z. Liu, and Q. Tian, "Query-adaptive late fusion for image search and person re-identification," in *IEEE Conf. Comput. Vis. Pattern Recognit.*, 2015, pp. 1741–1750.
- [11] W. Li, R. Zhao, T. Xiao, and X. Wang, "Deepreid: Deep filter pairing neural network for person re-identification," in *IEEE Conf. Comput. Vis. Pattern Recognit.*, 2014, pp. 152–159.
- [12] T. Xiao, H. Li, W. Ouyang, and X. Wang, "Learning deep feature representations with domain guided dropout for person re-identification," in *IEEE Conf. Comput. Vis. Pattern Recognit.*, 2016, pp. 1249–1258.
- [13] C. Su, J. Li, S. Zhang, J. Xing, W. Gao, and Q. Tian, "Pose-driven deep convolutional model for person re-identification," in *Int. Conf. Comput. Vis.*, 2017, pp. 3960–3969.
- [14] S.-Z. Chen, C.-C. Guo, and J.-H. Lai, "Deep ranking for person re-identification via joint representation learning," *IEEE Trans. Image Process.*, vol. 25, no. 5, pp. 2353–2367, 2016.
- [15] F. Zhu, X. Kong, L. Zheng, H. Fu, and Q. Tian, "Part-based deep hashing for large-scale person re-identification," *IEEE Trans. Image Process.*, vol. 26, no. 10, pp. 4806–4817, 2017.
- [16] H. Yao, S. Zhang, R. Hong, Y. Zhang, C. Xu, and Q. Tian, "Deep representation learning with part loss for person re-identification," *IEEE Trans. Image Process.*, 2019.
- [17] L. Zheng, Y. Huang, H. Lu, and Y. Yang, "Pose invariant embedding for deep person re-identification," *IEEE Trans. Image Process.*, 2019.
- [18] Y. Cai, V. Takala, and M. Pietikainen, "Matching groups of people by covariance descriptor," in *Int. Conf. Pattern Recognit.*, 2010, pp. 2744–2747.
- [19] W.-S. Zheng, S. Gong, and T. Xiang, "Associating groups of people," in *British Mach. Vis. Conf.*, 2009.
- [20] F. Zhu, Q. Chu, and N. Yu, "Consistent matching based on boosted saliency channels for group re-identification," in *IEEE Int. Conf. Image Process.*, 2016, pp. 4279–4283.
- [21] L. A. Gatys, A. S. Ecker, and M. Bethge, "Image style transfer using convolutional neural networks," in *IEEE Conf. Comput. Vis. Pattern Recognit.*, 2016, pp. 2414–2423.
- [22] J. Johnson, A. Alahi, and L. Fei-Fei, "Perceptual losses for real-time style transfer and super-resolution," in *European Conf. Comput. Vis.*, 2016, pp. 694–711.
- [23] K. Bousmalis, N. Silberman, D. Dohan, D. Erhan, and D. Krishnan, "Unsupervised pixel-level domain adaptation with generative adversarial networks," in *IEEE Conf. Comput. Vis. Pattern Recognit.*, 2017, pp. 3722–3731.
- [24] Y. Taigman, A. Polyak, and L. Wolf, "Unsupervised cross-domain image generation," *arXiv preprint arXiv:1611.02200*, 2016.
- [25] W. Deng, L. Zheng, Q. Ye, G. Kang, Y. Yang, and J. Jiao, "Image-image domain adaptation with preserved self-similarity and domain-dissimilarity for person re-identification," in *IEEE Conf. Comput. Vis. Pattern Recognit.*, 2018, pp. 994–1003.
- [26] C.-Y. Weng, W.-T. Chu, and J.-L. Wu, "Rolenet: Movie analysis from the perspective of social networks," *IEEE Trans. Multimedia*, pp. 256–271, 2009.
- [27] C.-M. Tsai, L.-W. Kang, C.-W. Lin, and W. Lin, "Scene-based movie summarization via role-community networks," *IEEE Trans. Circuits Syst. Video Technol.*, pp. 1927–1940, 2013.
- [28] E. Ristani, F. Solera, R. Zou, R. Cucchiara, and C. Tomasi, "Performance measures and a data set for multi-target, multi-camera tracking," in *European Conf. Comput. Vis. Workshop*, 2016, pp. 17–35.
- [29] L. Zheng, L. Shen, L. Tian, S. Wang, J. Wang, and Q. Tian, "Scalable person re-identification: A benchmark," in *IEEE Conf. Comput. Vis. Pattern Recognit.*, 2015, pp. 1116–1124.
- [30] J.-Y. Zhu, T. Park, P. Isola, and A. A. Efros, "Unpaired image-to-image translation using cycle-consistent adversarial networks," in *IEEE Conf. Comput. Vis. Pattern Recognit.*, 2017, pp. 2223–2232.
- [31] K. He, X. Zhang, S. Ren, and J. Sun, "Deep residual learning for image recognition," in *IEEE Conf. Comput. Vis. Pattern Recognit.*, 2016, pp. 770–778.